
A formulation of the non linear discrete Kirchhoff quadrilateral shell element with finite rotations and enhanced strains

Fakhreddine Dammak* — Said Abid**
Augustin Gakwaya*** — Gouri Dhatt****

* U2MP, Unité de mécanique, Modélisation et Production
Département de génie mécanique, ENIS, Sfax, 3038, Tunisie

** U2MP, Unité de mécanique, Modélisation et Production
Département de Technologie, IPEIS, Sfax, BP 805, 3018 Sfax Tunisie

*** Département de génie mécanique
Université Laval, Québec, G1K 7P4, Canada

**** Université de Technologie de Compiègne, UTC
Dépt. GSM, Division MNM, BP 529, F-60205, Compiègne

ABSTRACT. This paper presents a new formulation of the non-linear discrete Kirchhoff quadrilateral shell element applicable for the analysis of geometrically nonlinear structures undergoing finite rotations. The shell director is directly interpolated and the exact linearization of the discrete form of the equilibrium equations is derived in closed form. The consistent tangent stiffness matrix is symmetric and is given explicitly in this paper. Two or three rotational variables are used at each node. To improve the in-plane deformation enhanced incompatible modes are introduced. The formulation is then illustrated by a comprehensive set of numerical experiments selected from the literature.

RÉSUMÉ. Ce papier présente une nouvelle formulation de l'élément de coque quadrilatéral de type Kirchhoff discret non linéaire applicable à l'analyse des structures géométriquement non linéaires avec des rotations finies. Le vecteur directeur de la coque est interpolé directement et la linéarisation exacte de la forme discrète des équations de l'équilibre est dérivée d'une façon exacte. La matrice tangente consistante est symétrique, elle est donnée explicitement dans ce papier. Deux ou trois variables de rotation sont utilisées à chaque nœud. Pour améliorer les déformations dans le plan, des modes incompatibles sont introduits. La formulation est donc illustrée par un ensemble complet d'expériences numériques sélectionnées de la littérature.

KEYWORDS: nonlinear shell element, finite rotation, enhanced assumed strain.

MOTS-CLÉS : élément de coque non linéaire, grandes rotations, déformations enrichies supposées.

1. Introduction

Large efforts have been made in recent years to develop finite elements for the analysis of shell structures subjected to large displacements and rotations. Examples of them are those proposed in (Saleeb *et al.*, 1990; Parisch, 1991) where the classical degerated concept is revisited in nonlinear setting to incorporate the exact rotation updates, (Buechter *et al.*, 1991; Buechter *et al.*, 1992), where a comparison between classical shell theory and degerated approach, (Sansour *et al.*, 1992; Wriggers *et al.*, 1993) where non linear shell theories based on Biot formulation are explored and (Buechter *et al.*, 1994; Parisch, 1995) where an extension of nonlinear shell formulation to continuum three dimension is investigated. Other shell formulations based on the classical one director non-linear shell theory, considered in this work, are presented in (Simo *et al.*, 1990a; 1993a; Ibrahimbegovic, 1995; 1997) among others. All this development has been made on the kinematics hypothesis of Reissner-Mindlin.

In this paper, the non linear finite shell element in developed starting from the non linear classical shell theory where the Kirchhoff-Love constraint is applied in a discreet form.

The Kirchhoff-Love hypothesis consists in annulling the transverse shear deformation. This hypothesis requires a C^1 continuity for a compatible displacement model. This model, which only applies for the thin structures, has been used by several authors to develop linear and non-linear elements. The continuity C^1 , that requires the specification of the transverse displacement and all its derivatives at nodes, is very difficult to assure. To avoid these difficulties, several approaches have been proposed.

A first approach is based on an independent interpolation of variables of rotation and displacement. The hypothesis of Kirchhoff_Love is introduced then on the element boundaries or inside elements under collocation or integration form. One then recovers the family of the effective discreet Kirchhoff plate and shell elements: three nodes elements DKT: *Discreet Kirchhoff Triangle* (Dhatt, 1969; Batoz *et al.*, 1980; Kui, *et al.*, 1985; Dhatt *et al.*, 1986; Zienkiewicz *et al.*, 1990; Talaslidis *et al.*, 1992) and four nodes elements DKQ: *Discreet Kirchhoff Quadrilateral* (Batoz *et al.*, 1982; Jeyachandrabose *et al.*, 1987; Ibrahimbegovic, 1993; Krätzig *et al.*, 1994; Soh *et al.*, 2000; Razaqpur *et al.*, 2003).

In a second approach, to ensure C^1 continuity, one finds the class of elements based on the mixed formulations. We mention here, as an example, mixed/hybrid element HSM: *Hybrid Stress Model* (Batoz *et al.*, 1980) and the non-conforming displacement element of (Morley, 1991; Keulen *et al.*, 1993a; 1993b). These elements, HSM and the one of Morley, are among the simplest elements of Kirchhoff-Love type that pass the patch test of constant curvature with a number reduces degrees of freedom. On the other hand, the inconvenience of these elements resides of the presence of degrees of freedom on mid-side element boundaries. One

finds in (Hughes, 1987; Batoz *et al.*, 1990; Zienkiewicz *et al.*, 1991) more details formulations on the Kirchhoff plate and shell elements in the linear case.

In the case of nonlinear discrete Kirchhoff shell elements, most of papers deal with the three nodes element (Fafard *et al.*, 1989; Morley, 1991; Peng *et al.*, 1992; Keulen *et al.*, 1993a, 1993b; Bédouani *et al.*, 1995). For the four nodes elements, one finds the work of (Jaamei *et al.*, 1989) where the others use Marguerre theory but there is no reference to finite rotation.

In this paper, the non-linear finite element formulation presented is based on the four nodes discret Kirchhoff-Love element, DKQ where Kirchhoff-Love constrain is imposed under integral form on the element boundaries. Large rotations effects are included in this element.

Since it is known that finite element base upon low order isoparametric displacement formulation exhibit poor performance in bending and locking in the near incompressible limit, an enhanced assumed strains is introduced to improve the performances of the proposed non linear shell element. The assumed strain formulation is preferred to the assumed stress due to their natural compatibility with the strain driven format typically found in the algorithmic development of nonlinear materials (Simo *et al.*, 1990b, 1992, 1993b; Andelfinger *et al.*, 1993; Korelc *et al.*, 1997).

The paper is outlined as follows. In section 2 the governing equation is given as well as the variational formulation for the shell model which is then cast into its weak form. Finite element formulation is introduced in section 3 and the transformation relations and updating for the mixed enhanced assumed strain are presented in section 4. Representative numerical verifications are presented in section 5. Finally in section 6, conclusions are drawn and further work outlined.

2. Governing equation and weak form

It is well established that the local form of the equilibrium equation in terms of stress and stress couple resultants can be written (Simo *et al.*, 1990a):

$$\frac{1}{\bar{j}} \left(\bar{j} \mathbf{n}^\alpha \right)_{,\alpha} + \bar{\mathbf{n}} = \mathbf{0} \quad , \quad \frac{1}{\bar{j}} \left(\bar{j} \mathbf{m}^\alpha \right)_{,\alpha} - \mathbf{l} + \bar{\mathbf{m}} = \mathbf{0} \quad [1]$$

where \mathbf{n}^α and \mathbf{m}^α are the resultant stress and director couple resultants, $\bar{\mathbf{n}}$ and $\bar{\mathbf{m}}$ are the applied loads, \bar{j} is the surface Jacobien and \mathbf{l} is the cross the thickness stress resultant. Making use of the divergence theorem, one obtain the following expression of the weak form of the equilibrium equations:

$$G = \int_A (\mathbf{n} \cdot \delta \boldsymbol{\varepsilon} + \mathbf{m} \cdot \delta \boldsymbol{\rho} + \mathbf{q} \cdot \delta \boldsymbol{\gamma}) dA - G_{ext} = 0 \quad [2]$$

where G_{ext} is the external virtual work and given by

$$G_{ext} = \int_A (\bar{\mathbf{n}} \cdot \delta \boldsymbol{\varphi} + \bar{\mathbf{m}} \cdot \delta \mathbf{d}) dA + \int_{\partial A} (\mathbf{n}^\alpha \cdot \delta \boldsymbol{\varphi} + \mathbf{m}^\alpha \cdot \delta \mathbf{d}) \nu_\alpha \bar{j} d\Gamma \quad [3]$$

where $\delta \boldsymbol{\varphi}$ and $\delta \mathbf{d}$ are the variations associated to the position of the mid-surface and director field respectively, \mathbf{n} , \mathbf{m} and \mathbf{q} are components of the effective stress tensor (Simo *et al.*, 1990a) and are relative to the membrane, bending and transverse shear which can be written in matrix form as

$$\mathbf{n} = \bar{J} \begin{bmatrix} n^{11} \\ n^{22} \\ n^{12} \end{bmatrix}, \quad \mathbf{m} = \bar{J} \begin{bmatrix} m^{11} \\ m^{22} \\ m^{12} \end{bmatrix}, \quad \mathbf{q} = \bar{J} \begin{bmatrix} q_1 \\ q_2 \end{bmatrix} \quad [4]$$

where $\bar{J} = \bar{j} / \bar{j}_0$. $\delta \boldsymbol{\varepsilon}$, $\delta \boldsymbol{\rho}$ and $\delta \boldsymbol{\gamma}$ are the variations of shell strain

$$\begin{cases} \delta \varepsilon_{\alpha\beta} = 1/2 (\varphi_{,\alpha} \cdot \delta \varphi_{,\beta} + \varphi_{,\beta} \cdot \delta \varphi_{,\alpha}) \\ \delta \rho_{\alpha\beta} = 1/2 (\varphi_{,\alpha} \cdot \delta \mathbf{d}_{,\beta} + \varphi_{,\beta} \cdot \delta \mathbf{d}_{,\alpha} + \delta \varphi_{,\alpha} \cdot \mathbf{d}_{,\beta} + \delta \varphi_{,\beta} \cdot \mathbf{d}_{,\alpha}) \\ \delta \gamma_\alpha = \varphi_{,\alpha} \cdot \delta \mathbf{d} + \delta \varphi_{,\alpha} \cdot \mathbf{d} \end{cases} \quad [5]$$

From [5], we introduce the strain measures defined by:

$$\begin{cases} \varepsilon_{\alpha\beta} = 1/2 (\varphi_{,\alpha} \cdot \varphi_{,\beta} + \varphi_{\alpha,\alpha} \cdot \delta \varphi_{\alpha,\beta}) \\ \rho_{\alpha\beta} = 1/2 (\varphi_{,\alpha} \cdot \mathbf{d}_{,\beta} - \varphi_{\alpha,\alpha} \cdot \mathbf{d}_{\alpha,\beta}) \\ \gamma_\alpha = \varphi_{,\alpha} \cdot \mathbf{d} - \varphi_{\alpha,\alpha} \cdot \mathbf{d}_\alpha \end{cases} \quad [6]$$

and in matrix form

$$\boldsymbol{\varepsilon} = \begin{bmatrix} \varepsilon_{11} \\ \varepsilon_{22} \\ 2\varepsilon_{12} \end{bmatrix}, \quad \boldsymbol{\rho} = \begin{bmatrix} \rho_{11} \\ \rho_{22} \\ 2\rho_{12} \end{bmatrix}, \quad \boldsymbol{\gamma} = \begin{bmatrix} \gamma_1 \\ \gamma_2 \end{bmatrix} \quad [7]$$

In equations [5], $\delta \mathbf{d}$ and $\delta \mathbf{d}_{,\alpha}$ are the variation of the director and its derivative. These variations can be written either in spatial description

$$\delta \mathbf{d} = \delta \Theta \wedge \mathbf{d} = \bar{\Lambda} \delta \Theta, \quad \bar{\Lambda} = -\tilde{\mathbf{d}} \quad [8]$$

where $\tilde{\mathbf{d}}$ is the skew-symmetric tensor such that $\tilde{\mathbf{d}} \mathbf{d} = \mathbf{0}$,

or in material description

$$\delta \mathbf{d} = \Lambda \delta \tilde{\Theta} \mathbf{E}_3 = \bar{\Lambda} \delta \Theta, \quad \bar{\Lambda} = -\Lambda \tilde{\mathbf{E}}_3 \quad [9]$$

where we assumed that $\mathbf{d} = \Lambda \mathbf{E}_3$. It is shown in (Simo, 1993a) that with $\mathbf{E}_3 = [0 \quad 0 \quad 1]^t$, a spatial description leads to a shell problem with 6 DOF/node and the material description leads to a shell problem with 5 DOF/node, where the transformation $\bar{\Lambda}$ take the following form:

$$\bar{\Lambda} = \begin{bmatrix} -\mathbf{d}_2 & \mathbf{d}_1 \end{bmatrix}_{3 \times 2} \quad [10]$$

We next introduce the differential matrix operator \mathbf{B} , yet called the strain operator defined as

$$\mathbf{B} = \begin{bmatrix} \mathbf{B}_m \\ \mathbf{B}_b \end{bmatrix} \quad [11]$$

where \mathbf{B}_m and \mathbf{B}_b are membrane and bending strain operators

$$\mathbf{B}_m = \begin{bmatrix} \varphi_{,1}^t \frac{\partial}{\partial \xi} & \mathbf{0} \\ \varphi_{,2}^t \frac{\partial}{\partial \xi} & \mathbf{0} \\ \varphi_{,1}^t \frac{\partial}{\partial \xi} + \varphi_{,2}^t \frac{\partial}{\partial \xi} & \mathbf{0} \end{bmatrix} \quad [12]$$

$$\mathbf{B}_b = \begin{bmatrix} \mathbf{d}_{,1}^t \frac{\partial}{\partial \xi} & \varphi_{,1}^t \frac{\partial}{\partial \xi} \\ \mathbf{d}_{,2}^t \frac{\partial}{\partial \xi^2} & \varphi_{,2}^t \frac{\partial}{\partial \xi^2} \\ \mathbf{d}_{,1}^t \frac{\partial}{\partial \xi^2} + \mathbf{d}_{,2}^t \frac{\partial}{\partial \xi} & \varphi_{,1}^t \frac{\partial}{\partial \xi^2} + \varphi_{,2}^t \frac{\partial}{\partial \xi} \end{bmatrix} \quad [13]$$

Moreover, by defining the total resultant stress vector as

$$\mathbf{R} = \begin{bmatrix} \mathbf{n} \\ \mathbf{m} \end{bmatrix} \quad [14]$$

the weak form of the equilibrium equation in [2], with the Kirchhoff-Love constraint, can be rewritten as

$$G(\Phi, \delta\Phi) = \int_A \mathbf{R}^t \cdot \mathbf{B} \delta\Phi \, dA - G_{ext}(\Phi, \delta\Phi) = 0 \quad [15]$$

The last expression defines the nonlinear shell problem, which can be solved by the Newton iterative procedure. The consistent tangent operator for the Newton solution procedure can be constructed by the directional derivative of the weak form in the direction of the increment displacement and rotation $\Delta\Phi = (\Delta\varphi, \Delta\mathbf{d})$. It is a conventional practice to split the tangent operator into geometric and material parts, denoted by $D_G G \cdot \Delta\Phi$ and $D_M G \cdot \Delta\Phi$, respectively, *i.e.*,

$$DG \cdot \Delta\Phi = D_G G \cdot \Delta\Phi + D_M G \cdot \Delta\Phi \quad [16]$$

The geometric part results from the variation of the virtual strains while holding stress resultants constant. Accordingly, from [2] and [13], we obtain

$$D_G G \cdot \Delta\Phi = \int_A (\mathbf{n} \cdot \Delta\delta\varepsilon + \mathbf{m} \cdot \Delta\delta\rho) \, dA \quad [17]$$

where the corresponding components are given by

$$\Delta\delta\varepsilon_{\alpha\beta} = 1/2 \left(\Delta\varphi_{,\alpha} \cdot \delta\varphi_{,\beta} + \Delta\varphi_{,\beta} \cdot \delta\varphi_{,\alpha} \right) \quad [18]$$

$$\begin{aligned} \Delta\delta\rho_{\alpha\beta} = 1/2 \left(\Delta\varphi_{,\alpha} \cdot \delta\mathbf{d}_{,\beta} + \Delta\varphi_{,\beta} \cdot \delta\mathbf{d}_{,\alpha} + \delta\varphi_{,\alpha} \cdot \Delta\mathbf{d}_{,\beta} + \delta\varphi_{,\beta} \cdot \Delta\mathbf{d}_{,\alpha} \right) \\ + 1/2 \left(\varphi_{,\alpha} \cdot \Delta\delta\mathbf{d}_{,\beta} + \varphi_{,\beta} \cdot \Delta\delta\mathbf{d}_{,\alpha} \right) \end{aligned} \quad [19]$$

The material part of the tangent operator results from the variation in the stress resultants and thus takes the form

$$D_M G \cdot \Delta \Phi = \int_A \mathbf{B} \delta \Phi \cdot \Delta \mathbf{R} dA = \int_A \mathbf{B} \delta \Phi \cdot \mathbf{H}_T \cdot \mathbf{B} \Delta \Phi dA \quad [20]$$

where \mathbf{H}_T is the material tangent modulus which is given by the constitutive equations.

3. Finite element formulation

In this section, we elaborate the numerical implementation of the presented shell theoretical formulation base upon a four node non-linear shell element. It can be seen from [6] that the element geometry requires the position vector, as well as the associated shell director. Using the isoparametric concept, the variation and incremental position vector is approximated by

$$\delta \varphi = \sum_{I=1}^4 N^I \delta \varphi_I, \quad \Delta \varphi = \sum_{I=1}^4 N^I \Delta \varphi_I \quad [21]$$

where N_i are the standard isoparametric shape functions. For further details concerning isoparametric concept, we refer to standard references (Dhatt *et al.*, 1981; Hughes, 1987; Batoz *et al.*, 1990; Zienkiewicz 1991).

For the variation and increment director field, we choose a quadratic interpolation as the same one proposed in (Batoz *et al.*, 1990), to formulate linear discrete Kirchhoff plates elements.

$$\delta \mathbf{d} = \sum_{I=1}^4 N^I \delta \mathbf{d}_I + \sum_{K=5}^8 P_K \delta \alpha_K \mathbf{t}_K \quad [22]$$

$$\Delta \mathbf{d} = \sum_{I=1}^4 N^I \Delta \mathbf{d}_I + \sum_{K=5}^8 P_K \Delta \alpha_K \mathbf{t}_K \quad [23]$$

where (I) represent a node of the element, (K) represent the mid-point of the element boundaries and $\delta \alpha_K$ are variables associated to $\delta \mathbf{d}$ on the element boundaries. The vector \mathbf{t}_K is unit and its direction is defined by the position of the nodes couple (I, J) as shown in figure 1.

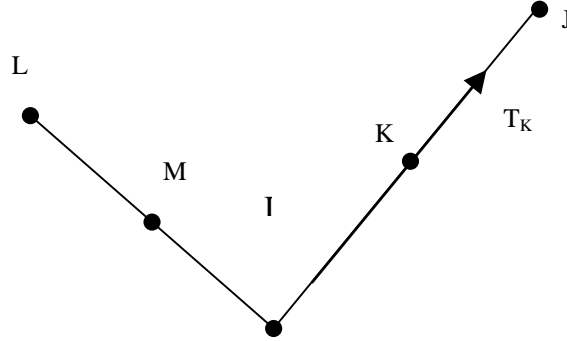


Figure 1. Position of the nodes couple (I, J)

$$\mathbf{t}_K = (\mathbf{x}_J - \mathbf{x}_I) / L_K, \quad L_K = \|\mathbf{x}_J - \mathbf{x}_I\| \quad [24]$$

where L_K is the I-J side length. The shape functions P_K are quadratic and are given in the Table 1.

Table 1. Functions P_K

P_K	$P_5 = 0.5(1 - \xi^2)(1 - \eta)$ $P_6 = 0.5(1 + \xi)(1 - \eta^2)$ $P_7 = 0.5(1 - \xi^2)(1 + \eta)$ $P_8 = 0.5(1 - \xi)(1 - \eta^2)$
-------	---

With these interpolations at hand, one can compute the discrete strain operator, residual and geometric matrix for membrane and bending.

3.1. Membrane deformation

We first consider the shell membrane part of the problem. At node (i), the associated strain matrix \mathbf{B}_m can be written as

$$\mathbf{B}_m^I = \begin{bmatrix} N_{,1}^I \varphi_{,1}^t & \mathbf{0} \\ N_{,2}^I \varphi_{,2}^t & \mathbf{0} \\ N_{,2}^I \varphi_{,1}^t + N_{,1}^I \varphi_{,2}^t & \mathbf{0} \end{bmatrix} \quad [25]$$

The corresponding contribution to the element residual is

$$\mathbf{R}_m = \int_A \mathbf{B}_m^t \cdot \mathbf{n} \, dA \quad [26]$$

The discrete approximation of the geometric tangent operator contributed by the membrane part associated with nodes (I, J) is then given by

$$\mathbf{GK}_m^{IJ} = \begin{bmatrix} \alpha^{IJ} \mathbf{I} & \mathbf{0} \\ \mathbf{0} & \mathbf{0} \end{bmatrix} \quad [27]$$

$$\alpha^{IJ} = \int_A \left(N_{,1}^I (n^{11} N_{,1}^J + n^{12} N_{,2}^J) + N_{,2}^I (n^{12} N_{,1}^J + n^{22} N_{,2}^J) \right) dA \quad [28]$$

3.2. Bending deformation

When one introduces the vanishing shearing hypothesis over the element boundaries under integral form, we have for side (I, J) :

$$\int_I^J \delta \gamma_{sz} \, ds = 0, \quad [29]$$

$$\delta \gamma_{sz} = \delta \beta_s + \delta \mathbf{u}_{,s} \cdot \mathbf{d}, \quad \delta \beta_s = \mathbf{t}_K \cdot \delta \mathbf{d} \quad [30]$$

where (s) is a parametric coordinate. While using a linear interpolation of the displacement vector $\delta \mathbf{u}$, this vector can be written for the side (I, J) as following :

$$\delta \mathbf{u} = (1 - \xi) \delta \mathbf{u}_I + \xi \delta \mathbf{u}_J, \quad 0 \leq \xi = s / L_K \leq 1 \quad [31]$$

The director vector \mathbf{d} is given by

$$\mathbf{d} = \frac{\tilde{\mathbf{d}}}{\|\tilde{\mathbf{d}}\|} \quad [32]$$

$$\delta \mathbf{d} = \frac{1}{\|\tilde{\mathbf{d}}\|} \mathbf{P}_d \delta \tilde{\mathbf{d}}, \quad \mathbf{P}_d = \mathbf{I} - \mathbf{d} \otimes \mathbf{d} \quad [33]$$

where \mathbf{P}_d is an orthogonal projection. Vector $\delta \tilde{\mathbf{d}}$ is defined by a quadratic interpolation as in equation [21]:

$$\delta \tilde{\mathbf{d}} = (1 - \xi) \delta \mathbf{d}_I + \xi \delta \mathbf{d}_J + 4\xi(1 - \xi) \delta \alpha_K \mathbf{t}_K \quad [34]$$

Then we have the final expression for the $\delta \beta_s$:

$$\delta \beta_s \approx \frac{1}{\|\tilde{\mathbf{d}}\|} \left((1 - \xi) \delta \beta_{sI} + \xi \delta \beta_{sJ} + 4\xi(1 - \xi) \delta \alpha_K \right) \quad [35]$$

Then to integrate the two terms of the vanishing shearing hypothesis, we use the relations [28], [29] and [32]. We can write after all made calculus:

$$\int_I \delta \mathbf{u}_{,s} \cdot \mathbf{d} \, ds \approx (\delta \mathbf{u}_I + \delta \mathbf{u}_J) \cdot \frac{(\mathbf{d}_I + \mathbf{d}_J)}{\|\mathbf{d}_I + \mathbf{d}_J\|} \quad [36]$$

$$\int_I \delta \beta_s \, ds \approx \frac{L_K}{\|\mathbf{d}_I + \mathbf{d}_J\|} \left(\delta \beta_{sI} + \delta \beta_{sJ} + \frac{4}{3} \delta \alpha_K \right) \quad [37]$$

The Kirchhoff-Love constraint is obtained by taking the sum of these last two equations equals to zero. This leads to the following expression of variables $\delta \alpha_k$:

$$\delta \alpha_K = \frac{3}{2L_K} \left((\delta \mathbf{u}_I + \delta \mathbf{u}_J) \cdot \mathbf{d}_K - \frac{3}{4} (\delta \mathbf{d}_I + \delta \mathbf{d}_J) \cdot \mathbf{t}_K \right) \quad [38]$$

$$\mathbf{d}_K = \frac{1}{2} (\mathbf{d}_I + \mathbf{d}_J) \quad [39]$$

One deducts from interpolation [21], the following expression of the vector :

$$\begin{aligned} \delta \mathbf{d} &= \sum_{I=1}^4 N^I \delta \mathbf{d}_I + \\ &\sum_{K=5}^8 \frac{3}{2} P_K (1/L_K (\delta \mathbf{u}_I + \delta \mathbf{u}_J) \cdot \mathbf{d}_K - 1/2 (\delta \mathbf{d}_I + \delta \mathbf{d}_J) \cdot \mathbf{t}_K) \mathbf{t}_K \end{aligned} \quad [40]$$

in a matrix form:

$$\delta \mathbf{d} = \sum_{I=1}^4 \mathbf{M}_d^I \delta \mathbf{u}_I + \mathbf{M}_r^I \delta \mathbf{d}_I \quad [41]$$

where matrixes \mathbf{M}_d^I and \mathbf{M}_r^I are given by the following expressions :

$$\mathbf{M}_d^I = P_K \mathbf{t}_K^I + P_M \mathbf{t}_M^I, \quad \mathbf{t}_K^I = \frac{3}{2L_K} \mathbf{t}_K \otimes \mathbf{d}_K \quad [42]$$

$$\mathbf{M}_r^I = N^I \mathbf{I} + P_K \mathbf{t}_K^I + P_M \mathbf{t}_M^I, \quad \mathbf{t}_K^I = \frac{3}{4} \mathbf{t}_K \otimes \mathbf{t}_K \quad [43]$$

The (K) and (M) are the two mid-side of every side of the quadrilateral, that are bound to the node (I) (figure 1).

Finally, the bending deformation, in the local Cartesian reference is expressed as:

$$\delta \rho = \mathbf{B}_b \delta \mathbf{U}_n \quad [44]$$

where

$$\mathbf{B}_b^I = \begin{bmatrix} \mathbf{B}_{bd}^I & \mathbf{B}_{br}^I \end{bmatrix} \quad [45]$$

$$\mathbf{B}_{bd}^I = \begin{bmatrix} \mathbf{d}_{,1}^I N_{,1}^I + \Phi_{,1}^I \cdot \mathbf{M}_{d,1}^I \\ \mathbf{d}_{,2}^I N_{,2}^I + \Phi_{,2}^I \cdot \mathbf{M}_{d,2}^I \\ \mathbf{d}_{,1}^I N_{,2}^I + \mathbf{d}_{,2}^I N_{,1}^I + \Phi_{,1}^I \cdot \mathbf{M}_{d,2}^I + \Phi_{,2}^I \cdot \mathbf{M}_{d,1}^I \end{bmatrix} \quad [46]$$

$$\mathbf{B}_{br}^I = \begin{bmatrix} \varphi_{,I}^t \mathbf{M}_{r,1}^I \\ \varphi_{,2}^t \mathbf{M}_{r,2}^I \\ \varphi_{,I}^t \mathbf{M}_{r,2}^I + \varphi_{,2}^t \mathbf{M}_{r,1}^I \end{bmatrix} \quad [47]$$

and the contribution to the element residual becomes

$$\mathbf{R}_b = \int_A \mathbf{B}_b^T \cdot \mathbf{m} \, dA \quad [48]$$

The discrete approximation for the geometric tangent operator contributed by bending part associated with nodes (I, J) is then given by

$$\mathbf{GK}_b^{IJ} = \begin{bmatrix} \mathbf{d}\mathbf{d}_b^{IJ} & \mathbf{d}\mathbf{r}_b^{IJ} \bar{\Lambda}_j \\ \bar{\Lambda}_i^t \mathbf{r}\mathbf{d}_b^{IJ} & \bar{\Lambda}_i^t \mathbf{r}\mathbf{r}_b^{IJ} \bar{\Lambda}_j \end{bmatrix} \quad [49]$$

where:

– Displacement terms are:

$$\mathbf{d}\mathbf{d}_b^{IJ} = \zeta_K^{IJ} \mathbf{t}\mathbf{d}_K^J - \zeta_M^{IJ} \mathbf{t}\mathbf{d}_M^J + \zeta_K^{II} \mathbf{t}\mathbf{d}_K^{1t} - \zeta_M^{II} \mathbf{t}\mathbf{d}_M^{1t} \quad [50]$$

$$\zeta_K^{IJ} = \int_A \left(P_{K,1}^J (m^{11} N_{,1}^I + m^{12} N_{,2}^I) + P_{K,2}^J (m^{12} N_{,1}^I + m^{22} N_{,2}^I) \right) dA \quad [51]$$

– Coupling terms are:

$$\mathbf{d}\mathbf{r}_b^{IJ} = \omega^{IJ} \mathbf{I} - \zeta_K^{IJ} \mathbf{t}\mathbf{t}_K^J - \zeta_M^{IJ} \mathbf{t}\mathbf{t}_M^J \quad [52]$$

$$\omega^{IJ} = \int_A \left(N_{,1}^J (m^{11} N_{,1}^I + m^{12} N_{,2}^I) + N_{,2}^J (m^{12} N_{,1}^I + m^{22} N_{,2}^I) \right) dA \quad [53]$$

$$\mathbf{r}\mathbf{d}_b^{IJ} = \mathbf{d}\mathbf{r}_b^{IJt}$$

– Rotation terms are:

$$\mathbf{r}\mathbf{r}_b^{IJ} = \mathbf{0} \quad \text{for } I \neq J \quad [54]$$

$$\mathbf{r}\mathbf{r}_b^{II} = -\chi_{II} \mathbf{I}, \quad \text{for } I=J \quad [55]$$

$$\chi_{II} = \left(\mathbf{V}^I - \mathbf{W}_K^{I'} \cdot \mathbf{t}_K^I - \mathbf{W}_M^{I'} \cdot \mathbf{t}_M^I \right) \mathbf{d}_I \quad [56]$$

$$\mathbf{V}^I = \int_A \left((m^{11} N_{,1}^I + m^{12} N_{,2}^I) \boldsymbol{\rho}_{,1} + (m^{12} N_{,1}^I + m^{22} N_{,2}^I) \boldsymbol{\rho}_{,2} \right) dA \quad [57]$$

$$\mathbf{W}_K^I = \int_A \left((m^{11} P_{K,1}^I + m^{12} P_{K,2}^I) \boldsymbol{\rho}_{,1} + (m^{12} P_{K,1}^I + m^{22} P_{K,2}^I) \boldsymbol{\rho}_{,2} \right) dA \quad [58]$$

This completes our development of the material and geometric tangents operators of the discrete Kirchhoff quadrilateral. We remark that as far as we are aware, the expression of the tangent matrix appears not to have been recorded previously in the literature.

4. Enhanced assumed strains

To improve the membrane behavior of the bilinear shell element, especially for in-plane bending dominated case; we enhance the compatible in-plane strain. With a field α :

$$\boldsymbol{\varepsilon} = \boldsymbol{\varepsilon}^c + \boldsymbol{\varepsilon}^{inc}, \quad \boldsymbol{\rho} = \boldsymbol{\rho}^c \quad [59]$$

$$\delta \boldsymbol{\varepsilon}^c = \mathbf{B}_m \delta \Phi, \quad \delta \boldsymbol{\varepsilon}^{inc} = \tilde{\mathbf{B}}_m \delta \alpha, \quad \delta \boldsymbol{\rho} = \mathbf{B}_{bb} \delta \Phi \quad [60]$$

The orthogonality condition is expressed as:

$$\int_A \boldsymbol{\varepsilon}^{inc \prime} \mathbf{n} dA = 0 \quad [61]$$

With this enhancement and the orthogonality condition, the three fields functional is rettin the as:

$$\pi = \int_A \frac{1}{2} \boldsymbol{\varepsilon}^t \mathbf{H}_m \boldsymbol{\varepsilon} dA + \int_A \boldsymbol{\varepsilon}^t \mathbf{H}_{mb} \boldsymbol{\rho} dA + \int_A \frac{1}{2} \boldsymbol{\rho}^t \mathbf{H}_{bb} \boldsymbol{\rho} dA \quad [62]$$

and its variation is:

$$G_{int} = \int_A \delta \boldsymbol{\varepsilon}^t \hat{\mathbf{n}} dA + \int_A \delta \boldsymbol{\rho}^t \hat{\mathbf{m}} dA \quad \left\{ \begin{array}{l} \boldsymbol{\varepsilon} = \boldsymbol{\varepsilon}^c + \boldsymbol{\varepsilon}^{inc} \\ \hat{\mathbf{n}} = \mathbf{H}_m \boldsymbol{\varepsilon} + \mathbf{H}_{mb} \boldsymbol{\rho} \\ \hat{\mathbf{m}} = \mathbf{H}_{mb} \boldsymbol{\varepsilon} + \mathbf{H}_{bb} \boldsymbol{\rho} \end{array} \right. \quad [63]$$

Further, after local condensation of parameter α we obtain:

$$\mathbf{A} = \int_A \mathbf{B}_m^t (\mathbf{H}_m \mathbf{B}_m + \mathbf{H}_{mb} \mathbf{B}_b) dA + \int_A \mathbf{B}_b^t (\mathbf{H}_{mb} \mathbf{B}_m + \mathbf{H}_{bb} \mathbf{B}_b) dA \quad [64]$$

$$\mathbf{B} = \int_A \tilde{\mathbf{B}}_m^t (\mathbf{H}_m \mathbf{B}_m + \mathbf{H}_{mb} \mathbf{B}_b) dA, \quad \mathbf{C} = \int_A \tilde{\mathbf{B}}_m^t \mathbf{H}_m \tilde{\mathbf{B}}_m dA \quad [65]$$

$$\Delta \alpha = -\mathbf{C}^{-1} (\mathbf{R} + \mathbf{B} \Delta \Phi) \quad [66]$$

The contribution of the element material tangent stiffness can then be computed as

$$\mathbf{K}_m = \mathbf{A} - \mathbf{B}^t \mathbf{C}^{-1} \mathbf{B} \quad [67]$$

The element geometric tangent stiffness is identical to displacement tangent element.

5. Numerical verification

In all verification tests treated in this section, we denote by MITC4, the Simo *and al.*, 1990a) element with the displacement formulation used for membrane and bending and assumed natural strain for shear. We denoted by SDK4 and SDK4I the four node discrete Kirchhoff shell element proposed in this paper with displacement and enhanced formulation.

The performance of the shell elements SDK4 and SDK4I is evaluated on several non-linear problems, selected from the literature, that encompass a wide range of deformation states involving warping, large rotations and large displacements.

5.1. Bending of a tapered beam

This example witch consist on a tapered beam subjected to an end load, serves to demonstrate the performance of the enhanced formulation versus the displacement formulation. J2 flow plasticity with isotropic hardening material is assumed with the following material properties: Young modulus $E=70$, Poisson 's ratio $\nu=1/3$, uniaxial tensile yield stress $\sigma_y=0.243$ and hardening modulud $H=0.2$. The Loading is increased in increments of $\Delta F = 0.1$ until a final value of 1.8 is reached. Initial and deformed configurations are shown in figure 2 for the SKQ4I element. figure 3 shows the vertical displacement of the top right node plotted versus number of element per side at the load level of $F=1.8$. computed with the SDK4 and SDK4I elements. In this test the geometric part is excuded. As demonstrated in figure 3, for this problem, SDK4 exhibits a significant degradation in accuracy over the mixed element SDK4I.

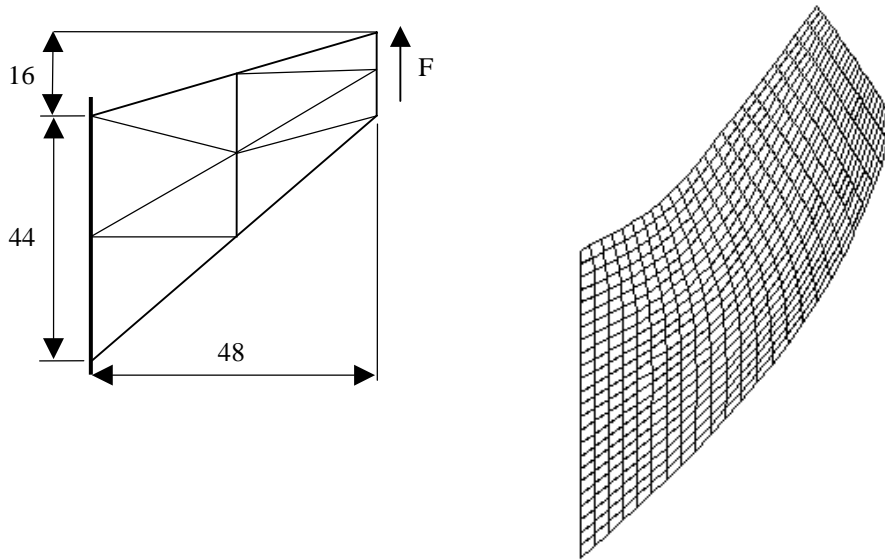


Figure 2. Initial and deformed configurations

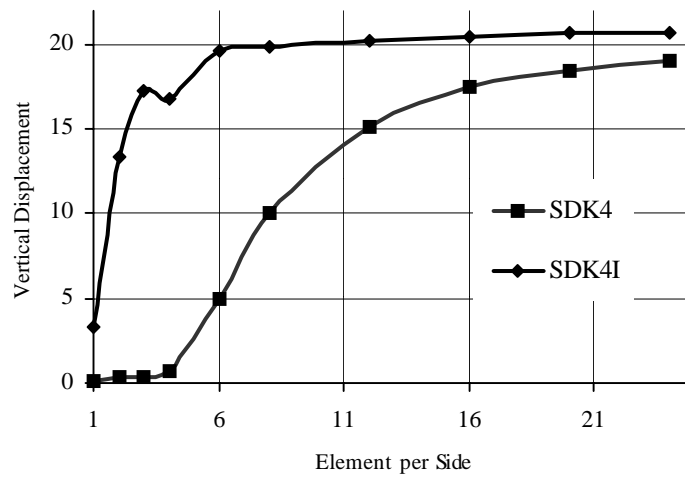


Figure 3. Load-deflection curves

5.2. Torsion of a flat plate strip

The purpose of this example is to demonstrate the ability of the formulation to capture large rotations. An initially flat shell clamped on one end is subjected to a torsional moment on the other end leading to a relative rotation of $\approx 180^\circ$. The initial and deformed configurations are shown in figure 4. The material properties are $E=12 E6$ and $\nu=0.3$. The plate length is $L=1.0$, the width is $w=0.25$ and the thickness is $t=0.1$. The final configuration is attained in three load steps.

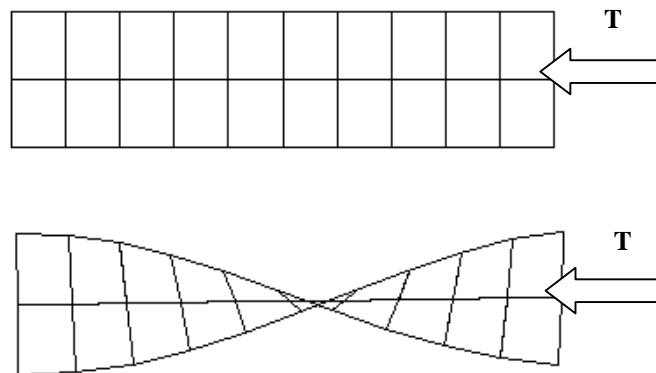


Figure 4. Initial and deformed configurations for the torsion of clamped plate

5.3. A pinched hemisphere

This numerical simulation is concerned with some analysis of the non-linear response of a pinched hemispherical shell with a 18° hole at the top and two inward and outward forces 90° apart. This test is given in (Simo *et al.*, 1990a) with four node quadrilateral elements. This problem is an excellent test of the ability of an element to handle finite rotations. The radius is $R=10$, the thickness $h=0.04$ and material properties are: $E=12 \times 10^6$ and $\nu=0.3$. The total load $F=100$ is applied in 5 equal increments. Using symmetry boundary conditions, one quadrant of the shell is modeled with 4×4 , 8×8 and 16×16 quadrilateral elements. The initial and deformed configurations for 16×16 meshing are shown in figure 5 and 6 and the load-deflection plots at the points of the application of the loads are shown in figure 7 and 8. The results for SDK4 and SDK4I are in complete agreement with those obtained using the results based element MITC4.

Since we have developed an exact expression for the tangent operator, the Newton method solution procedure exhibits an asymptotic rate of convergence. This rate was observed in all the problems examined. As an illustration, we record in Table 2. the value of the energy norm obtained during the fifth load step. The same

asymptotic rate of convergence is observed with both MITC4, SDK4 and SDK4I elements.

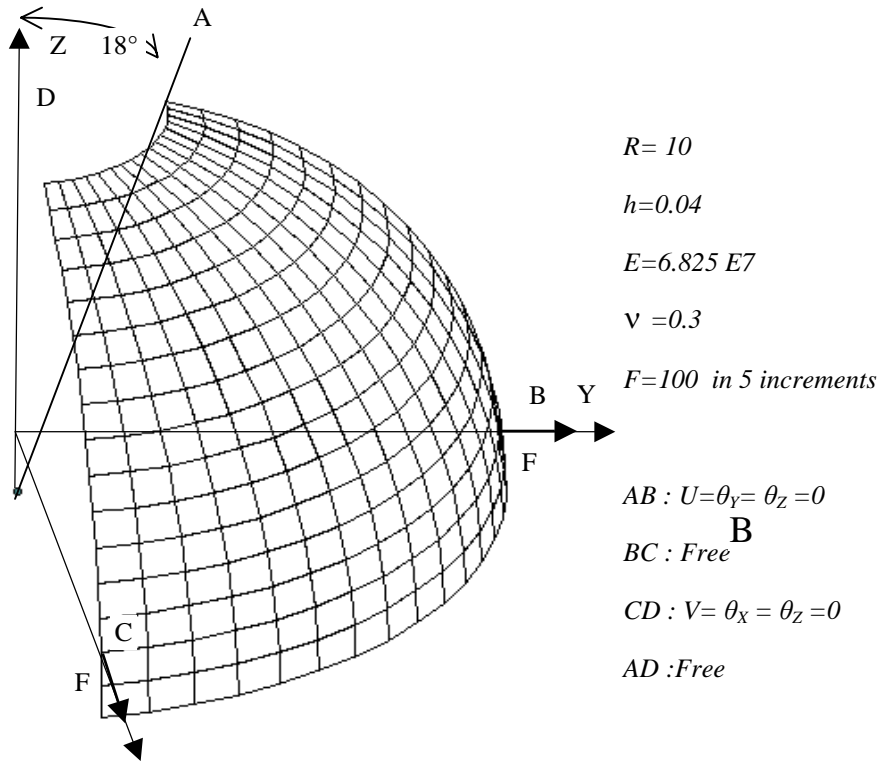


Figure 5. Initial mesh configurations for the pinched hemisphere

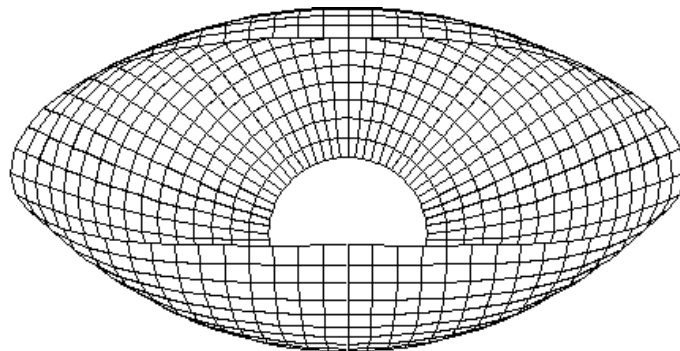


Figure 6. Deformed mesh configurations for the pinched hemisphere

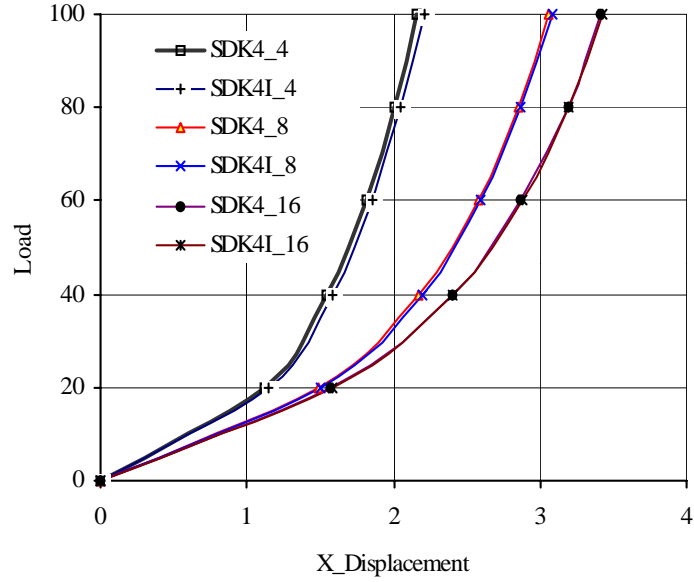


Figure 7. Load-X_displacement for the different mesh configurations

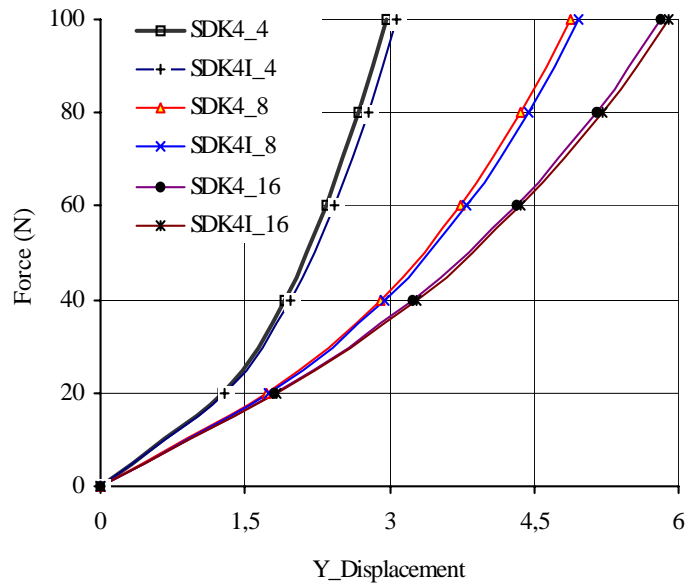


Figure 8. Load-Y_displacement for the different mesh configurations

Table 2. A pinched hemisphere Convergence at th 5th load step

Iterations	SDK4	SDK4I	MITC4
1	0.1000E+1	0.1000E+1	0.1000E+1
2	0.2707E+3	0.2824E+3	0.3077E+3
3	0.3738E-1	0.4040E-1	0.4144E-1
4	0.1468E-2	0.1614E-2	0.3865E-2
5	0.3446E-3	0.4459E-3	0.3178E-2
6	0.3308E-5	0.1764E-5	0.1555E-4
7	0.8016E-8	0.4290E-8	0.6477E-7
8	0.1492E-11	0.8302E-11	0.7396E-14
9	0.2293E-13	0.2042E-13	0.3154E-22
10	0.6509E-16	0.4645E-16	---

5.4. Hyperboloidal composite shell under two pairs of opposites loads

Finally, this example (figure 9) has to demonstrate the applicability of the proposed shell models to arbitrary composite shell geometries and strong nonlinearities.

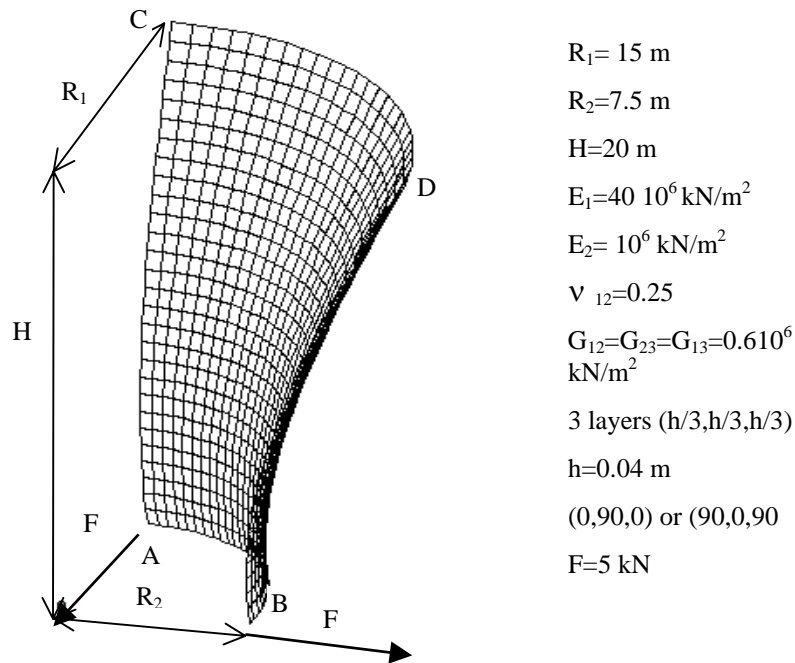


Figure 9. Hyperboloidal composite shell under two pairs of opposites loads

Due to the symmetry only one eighth of the shell is discretized. The shell has been analyzed for two set of laminate schemes 0/90/0 and 90/0/90.

In the figure 10 we show the deformed shape for this two laminate schemes. These figures demonstrate the considerable influence of the lamination arrangement on the deformation behaviour. The corresponding results illustrated in figure 11 and 12 for the displacement of the characteristic points A, B, C and D including results due to (Basar *et al.*, 1993) with a Mindlin-Reissner shell element.

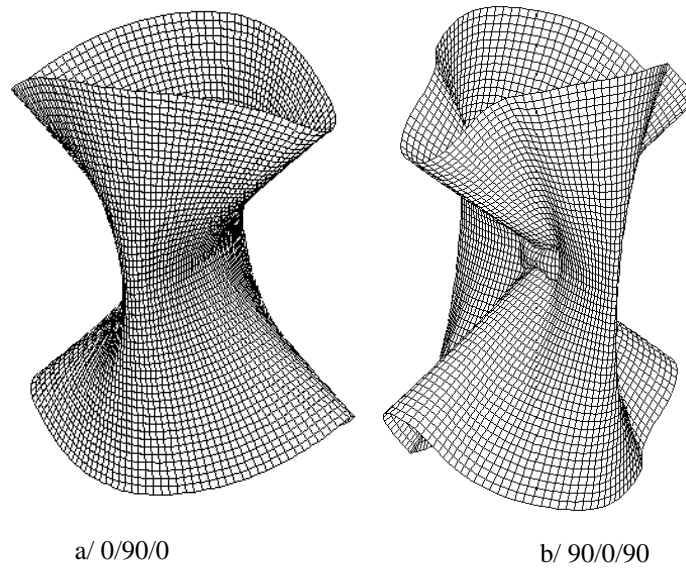


Figure 10. Deformed mesh configurations for the load level $f=32.0$

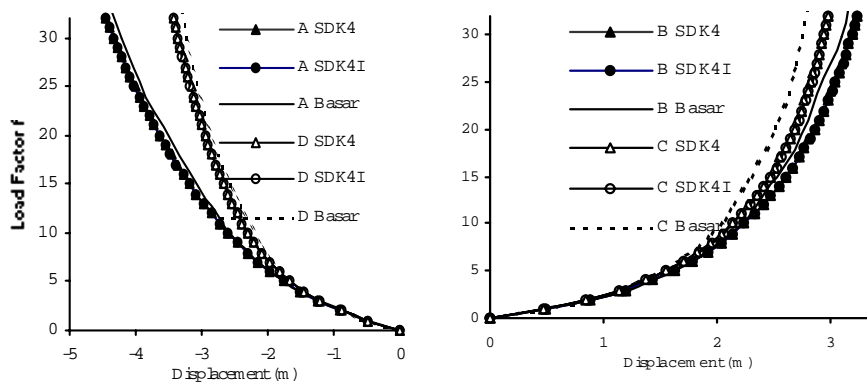


Figure 11. Hyperboloidal composite shell 0/90/0, Load-displacement at A,B,C,D

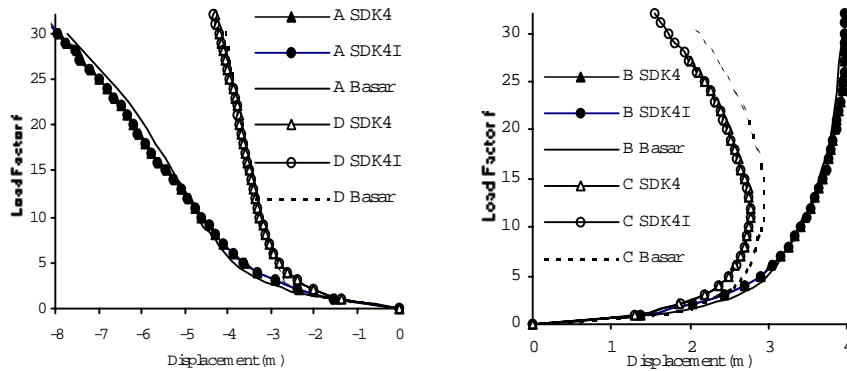


Figure 12. Hyperboloidal composite shell 90/0/90, Load-displacement at A,B,C,D

6. Conclusions

In this paper we are derived a new formulation of the non-linear discrete Kirchhoff quadrilateral shell element for the analysis of geometrically nonlinear structures. The element allows the occurrence of finite rotations. The shell director is directly interpolated and the exact linearization of the discrete form of the equilibrium equations is derived in closed form. An enhanced incompatible modes are introduced to improve the in-plane deformations. Examples show the applicability and effectivity of the developed element.

In the proposed formulation of the non-linear discrete Kirchhoff quadrilateral shell element, the Kirchhoff constraint is taken at each iteration. The rotations updating at nodes are the same one used in a Mindlin formulation (Appendix Table 3). At mid-side the updating of rotations is made consistent with the Kirchhoff constraint (Appendix Table 4). According to our experience, the response of the proposed element formulation converges to Kirchhoff theory. However, a little slower convergence can be observed in some cases compared to the Mindlin element MITC4 (Table 2). This can be due to the rotations mid-side updating where we use the nodal displacements solution to compute the mid-side rotations $\Delta\alpha$ as obtained from the Kirchhoff constraint. A deepened survey should be considered on this topic.

7. References

- Andelfinger U., Ramm E., "EAS-Element for two dimensional, three-dimensional, plate and shell structures and their equivalence to HR-elements", *Int. J. Numer. Meth. Eng.*, 36, 1993, pp. 1311-1337.

- Basar Y., Ding Y., Schltz R., "Refined shear-deformation models for composite laminates with finite rotations", *Int. J. Solids Struct.*, 30, 1993, pp. 2611-2638.
- Batoz J. L., Bathe K. J., Ho L. W., "A study of three-node triangular plate bending elements", *Int. J. Numer. Meth. Eng.*, 15, 1980, pp. 1771-1812.
- Batoz J. L., Ben Taher M., "Evaluation of a new quadrilateral thin plate bending element", *Int. J. Numer. Meth. Eng.*, 18, 1982, pp. 1655- 1677.
- Batoz J. L., Dhatt G., *Modélisation des structures par éléments finis*, vol. 1, 2, 3, Hermès, Paris, 1990.
- Bédouani M. C., Tallec P. L., Mouro J., "Approximations par éléments finis d'un modèle de coques minces géométriquement exact", *Revue européenne des éléments finis*, 4, 1995, pp. 632-661.
- Betsch P., Gruttmann F., Stein E., "A 4-node finite shell element for the implementation of general hyperelastic 3D-elasticity at finite strains", *Computer Methods in Applied Mechanics and Engineering*, 130, 1996, pp. 57-79.
- Brank B., Peric D., Damijaic F. B., "On large deformation of thin elasto-plastic shells: implementation of finite rotation model for quadrilateral shell element", *Int. J. Numer. Meth. Eng.*, 40, 1997, pp. 689-726.
- Briassoulis D., "Non-linear behaviour of the RFNS element-large displacements and rotations", *Computer Methods in Applied Mechanics and Engineering*, 192, 2003, pp. 2909-2924.
- Buechter N., Ramm E., Large rotation in Structural Mechanics, Centre international des sciences mécaniques (CISM), Udine, Italy, June 24-28, 1991.
- Buechter N., Ramm E., "Shell theory versus dgeneration – A Comparison in large rotation finite element analysis", *Int. J. Numer. Meth. Eng.*, 34, 1992, pp. 39-59.
- Buechter N., Ramm E., Roehl D., "Three dimensional extension of non-linear shell formulation based on the enhanced assumed strain concept", *Int. J. Numer. Meth. Eng.*, 37, 1994, pp. 2551-2568.
- Dhatt G., "Numerical analysis of thin shells by curved triangular elements based on discrete Kirchhoff hypothesis", *proc ASCE Symp. On applications of FEM in civil engineering*, Vanderbilt Univ, Nashville, Tenn, 1969, pp. 255-278.
- Dhatt G., Touzot G., *Une présentation de la méthode des éléments finis*, Maloine, S. A. Editeur Paris et Les Presses de l'Université Laval Québec, 1981.
- Dhatt G., Marcotte L., Matte Y., "A new triangular discrete Kirchhoff plate/shell element", *Int. J. Numer. Meth. Eng.*, 23, 1986, pp. 453-470.
- Fafard M., Dhatt G., Batoz J.-L., "A new discrete Kirchhoff plate/shell element with updated procedures", *Comp. Struct.*, 31, 1989, pp. 591-606.
- Hughes T. J. R., *The finite element method: linear static and dynamic finite element analysis*, Prentic Hall, 1987.
- Ibrahimbegovic A., "Assumed shear strain in finite rotation shell analysis", *Eng. Comput.*, 12, 1995, pp. 425-438.

- Ibrahimbegovic A., "Stress resultant geometrically exact shell theory for finite rotations and its finite element implementation", *ASME, Appl. Mech Reviews*, 50 (4), 1997, pp. 199-226.
- Ibrahimbegovic A., "Quadrilateral finite elements for analysis of thick and thin plates", *Comp. Methods Appl. Mech. Eng.*, 110, 1993, pp. 195-209.
- Jaamei S., Frey F., Jetteur P., "Nonlinear thin finite element with six degrees of freedom per node", *Comp. Methods Appl. Mech. Eng.*, 75, 1989, pp. 251-266.
- Jeyachandrabose C., Kirkhope J., Mickisho L., "An improved discrete Kirchhoff quadrilateral thin-plate bending element", *Int. J. Numer. Meth. Eng.*, 24, 1987, pp. 635-654.
- Keulen F. V., Bout A., Ernest L. J., "Nonlinear thin shell using curved triangular element", *Comp. Methods Appl. Mech. Eng.*, 103, 1993a, pp. 315-343.
- Keulen F. V., "A geometrically nonlinear curved shell element with constant resultants", *Comp. Methods Appl. Mech. Eng.*, 106, 1993b, pp. 315-352.
- Korelc J., Weiggers P., "Improved enhanced strain four node element with Taylor expansion of the shape function", *Int. J. Numer. Meth. Eng.*, 40, 1997, pp. 407-421.
- Krätzig W. B., Zhang J. W., "A simple four-node quadrilateral finite element for plates", *Journal of Computational and Applied Mathematics*, 50, 1994, pp. 361-373.
- Kui L. X., Liu G. Q., Zienkiewicz O. C., "A generalized displacement method for the finite element analysis of thin shells", *Int. J. Numer. Meth. Eng.*, 21, 1985, pp. 2145-2155.
- Morley L. S. D., "Geometrically non-linear constant moment triangle which passes the Von Karman path test", *Int. J. Numer. Meth. Eng.*, 31, 1991, pp. 241-263.
- Parisich H., "An investigation of a finite rotation four node assumed strain shell element", *Int. J. Numer. Meth. Eng.*, 31, 1991, pp. 127-150.
- Parisich H., "A continuum based shell theory for non linear applications", *Int. J. Numer. Meth. Eng.*, 38, 1995, pp. 1855-1883.
- Peng X., Crisfield M. A., "A consistent co-rotational formulation for shells using the constant stress/constant moment triangle", *Int. J. Numer. Meth. Eng.*, 35, 1992, pp. 1829-1847.
- Razaqpur A. G., Nofal M., Vasilescu A., "An improved quadrilateral finite element for analysis of thin plates", *Finite Elements in Analysis and Design*, 40, 2003, pp. 1-23.
- Saleeb A. F., Chang T. Y., Graf W., Yingyeunyong S., "A hybrid/mixed model for nonlinear shell analysis and its application to large-rotation problems", *Int. J. Numer. Meth. Eng.*, 29, 1990, pp. 407-446.
- Sansour C., Bufler H., "An exact finite rotation shell theory, its mixed variational formulation and its finite element implementation", *Int. J. Numer. Meth. Eng.*, 34, 1992, pp. 73-115.
- Simo J.-C., Rifai M. S., Fox D. D., "On a stress resultant geometrically exact shell model. Part III : Computational aspects of the nonlinear theory", *Comp. Methods Appl. Mech. Eng.*, 79, 1990a, pp. 21-70.
- Simo J.-C., Rifai M. S., "A class of mixed assumed strain methods and the methods of incompatible modes", *Int. J. Numer. Meth. Eng.*, 29, 1990b, pp. 1595-1638.

- Simo J.-C., Armero F., “Geometrically non-linear enhanced strain mixed methods and the method of incompatible modes”, *Int. J. Numer. Meth. Eng.*, 33, 1992, pp. 1413-1449.
- Simo J.-C., “On a stress resultants geometrically exact shell model. Part:VII: Shell intersection with 5/6 DOF finite element formulations”, *Comp. Methods Appl. Mech. Eng.*, 108, 1993a, pp. 319-339.
- Simo J.-C., Armero F., Taylor R. L., “Improved version of assumed enhanced strain tri-linear elements for 3D finite deformation problems”, *Comp. Methods Appl. Mech. Eng.*, 110, 1993b, pp. 359-386.
- Soh K., Long Z., Song C., “Development of a new quadrilateral thin plate element using area coordinates”, *Comp. Methods Appl. Mech. Eng.*, 190, 2000, pp. 979-987.
- Talasilidis D., Sous I., “A discrete Kirchoff triangular element for the analysis of thin stiffened shells”, *Comp. Struct.*, 43, 1992, pp. 663-674.
- Wriggers P., Gruttmann F., “Thin shells with finite rotations formulated in Biot stresses: Theory and finite element formulation”, *Int. J. Numer. Meth. Eng.*, 36, 1993, pp. 2049-2071.
- Zienkiewicz O. C., Taylor R. L., Papadopoulos P., E. Onate, “Plate bending element with discrete constraints: New triangular elements”, *Comp. Struct.*, 35, 1990, pp. 505-522.
- Zienkiewicz O. C., Taylor R. L., *The finite element method*, 4th Edition., vol. 1, 2, McGraw-Hill, London, 1991.

Appendix

Table 3. *Nodal Updates*

<ul style="list-style-type: none"> • Directors and matrix for 6ddl 	$\Delta \mathbf{d} = \Delta \boldsymbol{\theta} \wedge \mathbf{d}^k$ $\mathbf{d}^{k+1} = \cos(\Delta d) \mathbf{d}^k + \frac{\sin(\Delta d)}{\Delta d} \Delta \mathbf{d}, \quad \Delta d = \ \Delta \mathbf{d}\ $ $\bar{\mathbf{A}}^{k+1} = -\tilde{\mathbf{d}}^{k+1}$
<ul style="list-style-type: none"> • Directors and matrix for 5ddl 	$\Delta \mathbf{d} = \bar{\mathbf{A}}^k \Delta \boldsymbol{\theta}$ $\mathbf{d}^{k+1} = \cos(\Delta d) \mathbf{d}^k + \frac{\sin(\Delta d)}{\Delta d} \Delta \mathbf{d}, \quad \Delta d = \ \Delta \mathbf{d}\ $ $\Delta \boldsymbol{\theta} = \mathbf{d}^k \wedge \Delta \mathbf{d}, \quad \bar{\mathbf{A}}^{k+1} = \exp(\bar{\Delta \boldsymbol{\theta}}) \bar{\mathbf{A}}^k$

Table 4. *Mid-Side (K) director updates*

$$L_K = \|\mathbf{x}_J^k - \mathbf{x}_I^k\|$$

$$\Delta\alpha_K = \frac{3}{2L_K} \left((\Delta\mathbf{u}_I + \Delta\mathbf{u}_J) \cdot \mathbf{d}_K^k - \frac{3}{4} (\Delta\mathbf{d}_I + \Delta\mathbf{d}_J) \cdot \mathbf{t}_K^k \right)$$

$$\Delta\mathbf{d}_K = \frac{1}{2} (\Delta\mathbf{d}_I + \Delta\mathbf{d}_J) + \Delta\alpha_K \cdot \mathbf{t}_K^k$$

$$\mathbf{d}_K^{k+1} = \cos(\Delta d) \mathbf{d}_K^k + \frac{\sin(\Delta d)}{\Delta d} \Delta\mathbf{d}_K, \quad \Delta d = \|\Delta\mathbf{d}_K\|$$

Table 5. *Gauss Points Updates*

$$\Delta\mathbf{d} = \sum_I N^I \Delta\mathbf{d}_I + \sum_K P_K \Delta\alpha_K^k \mathbf{t}_K^k, \quad \Delta\mathbf{d}_{,\alpha} = \sum_I N_{,\alpha}^I \Delta\mathbf{d}_I + \sum_K P_{K,\alpha} \Delta\alpha_K^k \mathbf{t}_K^k$$

$$\mathbf{d}^{k+1} = \cos(\Delta d) \mathbf{d}^k + \frac{\sin(\Delta d)}{\Delta d} \Delta\mathbf{d}, \quad \Delta d = \|\Delta\mathbf{d}\|$$

$$\mathbf{d}_{,\alpha}^{k+1} = \cos(\Delta d) \mathbf{d}_{,\alpha}^k + \mathbf{T}^{k+1} \Delta\mathbf{d}_{,\alpha}$$
